## 6. ANTARCTICA

*a. Overview*—R. L. Fogt and T. A. Scambos

In comparison to other regions of the globe, detailing Antarctic climate variability is not an easy task, mainly due to the quantity and quality of available data. Atmospheric reanalysis datasets, which fill in large spatial data voids across Antarctica, are strongly dependent on satellite data (Bromwich et al. 2007), thereby effectively limiting large-scale climate analysis in the high southern latitudes to post-1979. In light of this comparatively short record, several interesting Antarctic climate anomalies during 2008 are described in this section.

Overall, the year was dominated by a positive phase of the Southern Hemisphere Annular Mode. There was strong warming along the Antarctic Peninsula and West Antarctica in 2008, most marked in September and December, and also pockets of warming along coastal East Antarctica. Moderate La Niña events occurred during the austral summers of 2007–08 and 2008–09, and the simultaneous occurrence of these events with positive SAM phases amplified the regional response in West Antarctica and the Antarctic Peninsula region (e.g., Fogt and Bromwich 2006). This is particularly noted in changes in sea-ice concentration in the Amundsen/Bellingshausen Seas, which continued to show decline in 2008, in concert with and possibly contributing to the warming of the region. Precipitation anomalies were also above normal along portions of the Antarctic Peninsula in austral spring due to the SAM/La Niña influence. The positive phase of the SAM led to record-high total Antarctic sea-ice extent for much of early 2008 through enhanced equatorward Ekman transport. With colder continental temperatures at this time, the 2007–08 austral summer snowmelt season was dramatically weakened, making it the second-shortest melt season since 1978 when the record began. The lower stratosphere was anomalously cold throughout the polar night, with the 2008 ozone hole being the sixth worst on record and unusually persistent.

Another significant event during 2008 was the disintegration and retreat of the Wilkins Ice Shelf in the southwest peninsula area (Fig. 6.1). Three breakup events took place: one near the end of the summer melt season (29 February to 6 March, Fig. 6.1a) and two more in the 2008 autumn and winter (27–31 May, Fig. 6.1b; 28 June to mid-July, Fig. 6.1c). The shelf lost 431 km$^2$ in the first event and 160 km$^2$ in the second, and it saw calving and rifting of nearly 6,000 km$^2$ in the winter event (out of a total area of 13,680 km$^2$ just prior to the breakups; Fig. 6.1). Analysis of the breakups and the evolution of the Wilkins Ice Shelf leading up to these events suggested either that melt- and brine-layer-driven enhancement of fracturing led to the retreats or that basal melting from warmer near-surface and sub-shelf ocean layers caused weakening of the ice plate (Scambos et al. 2009; Padman et al. 2009; Braun et al. 2008). A further suspected contributing factor is ocean wave action. The extended period of ice-free conditions near the Wilkins Ice Shelf for much of the first half of the year exposed the shelf front directly to the open ocean swell. All of these models and hypotheses point to the glaciological consequences of the continuing climate warming and sea-ice decline in the peninsula region.

There were also recent advances in Antarctic climate science during 2008, most notably in prominent papers in *Nature Geoscience* by Gillett et al. (2008) and in *Nature* by Steig et al. (2009). Gillett et al. (2008) analyze fully coupled climate model simulations and demonstrate that human activity has contributed

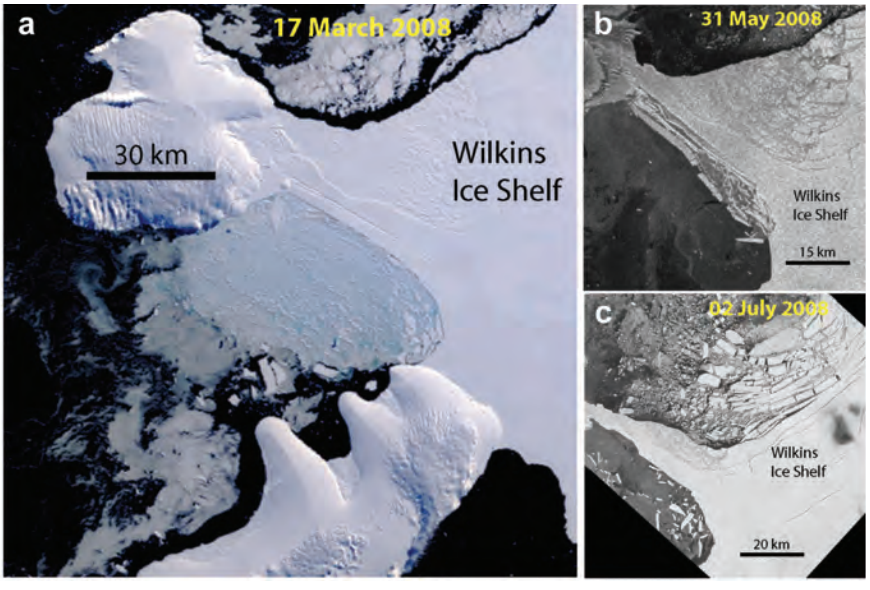


**Fig. 6.1. Wilkins Ice Shelf breakup events of 2008. (a) MODIS band 1 image 10 days after the end of the first event; (b) *Envisat* ASAR image during the second event; (c) *Envisat* ASAR image during the third event. (*Envisat* ASAR images © European Space Agency.)**

to the warming not only in the Arctic but also in the Antarctic. Steig et al. (2009) demonstrate that significant warming since the IGY (1957–58)—previously thought confined to the Antarctic Peninsula—is much broader in spatial extent, expanding to include West Antarctica. Additionally, a synthesis report (Mayewski et al. 2009) of the relevant mechanisms and long-term changes in the full Antarctic climate system also appeared recently. Such manuscripts help to place contemporaneous Antarctic climate variations described herein in the context of global climate change. However, the large interannual variability in the southern high latitudes complicates this matter by making trend detection difficult. Therefore, the record seasonal highs in Antarctic sea-ice extent in early and late 2008, for example, are not evidence against global change, because conclusions about long-term trends in Southern Hemisphere sea-ice extent cannot be drawn from monthly seasonal observations taken out of spatial and temporal contexts.

*b. Atmospheric circulation*—R. L. Fogt and S. Barreira

The large-scale Antarctic circulation anomalies during 2008 based on NCEP–NCAR reanalyses are highlighted through a zonal mean perspective, covering both the troposphere and stratosphere (Fig. 6.2), and spatially at the Antarctic surface (Fig. 6.3). During the beginning of the year (January–March), low geopotential height anomalies over high latitudes and strong zonal wind anomalies at midlatitudes throughout the troposphere and stratosphere were observed, indicative of the positive SAM phase. The lower-than-average surface pressures in the Antarctic circumpolar trough in this period (Fig. 6.3a) resulted from an increase in individual cyclonic activity, while the strengthened circumpolar westerly wind anomalies (Fig. 6.2c) aided in isolating the Antarctic continent from the warmer midlatitudes, generating the colder temperatures over most of coastal Antarctica (Fig. 6.3b). In many places, these temperature anomalies were more than two standard deviations below the January–March mean. During April–May, high pressure anomalies over Antarctica as well as throughout much of the Pacific Ocean, in conjunction with predominantly negative anomalies in the midlatitudes of the Eastern Hemisphere, generated only a weakly negative SAM index (Fig. 6.3c). The overall weaker circumpolar westerly winds (Fig. 6.2c) at this time allowed for more intrusions of warmer air from the north, leading to low-level warm temperature anomalies across much of the Antarctic continent, especially over East Antarctica (Figs. 6.2b, 6.3d). The pressure anomaly in the Amundesn/Bellingshausen Seas in Fig. 6.3c indicates that many low-pressure systems formed in this region; however, due to the presence of a strong high-pressure anomaly in the Pacific, they were impeded from traveling north toward South America.

A strong positive SAM anomaly occurred in June [3.00 on the Marshall (2003) index, the second-highest Jun positive SAM anomaly since 1957; www.antarctica.ac.uk/met/gjma/sam.html], with corresponding strong circumpolar winds (Fig. 6.2c). Throughout the remaining winter season, however,

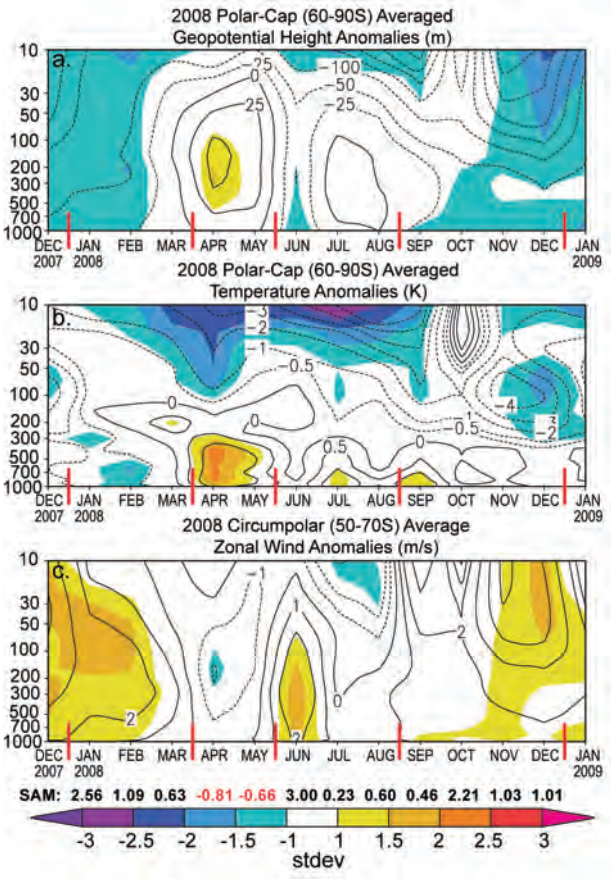


**Fig. 6.2. Zonally averaged climate parameter anomalies for the southern polar region in 2008 relative to the 1979–2007 period. (a) Polar cap averaged geopotential height anomalies (m); (b) averaged temperature anomalies (K); (c) averaged wind anomalies (m $s^{-1}$). Absolute anomaly values are contoured, and the panels are shaded according to how many std devs the anomalies are from the 1979–2007 mean (color bar at bottom for scale). Red vertical bars indicate the four separate periods shown as spatial climate anomalies for 2007 in Fig. 6.3. Primary contour interval is 50 m in (a), 1 K in (b), and 2 m $s^{-1}$ in (c), with additional contours at ±25m, ±0.5K, ±1 m $s^{-1}$ in (a), (b), and (c), respectively. Values for the SAM index (www.antarctica.ac.uk/met/gjma/sam.html) are shown along the bottom in black and red. Data are from the NCEP–NCAR reanalysis.**

the tropospheric circulation anomalies were relatively weak, although the pressure anomalies continued to indicate the positive phase of the SAM (Fig. 6.3e). At the end of the year (September–December), the positive SAM began to increase at the same time a La Niña began to develop in the tropics, peaking in December 2008. The simultaneous occurrence of positive SAM and La Niña was characterized by anomalously low geopotential height throughout the atmosphere and strong circumpolar zonal flow (Fig. 6.2), similar to the anomalies in December of 2007. At the surface, the low pressure anomalies (>2 std devs from the mean) were most marked in the Amundsen/Bellingshausen Seas, the region strongly influenced by both SAM and ENSO (Fig. 6.3g). The altered circulation brought stronger northwesterly flow to the Antarctic Peninsula and portions of West Antarctica, leading to the marked warming there (Fig. 6.3h), also more than two standard deviations above the late-year mean. In addition, the strong negative pressure anomalies in the South Pacific enhanced the off-continent flow in the eastern Ross Sea, leading to much cooler-than-normal conditions farther over the South Pacific Ocean. The strong ridge in the subtropical Atlantic deterred the low-pressure systems forming in the Amundesn/Bellingshausen Seas away from southern South America, leading to very dry conditions there at the end of 2008.

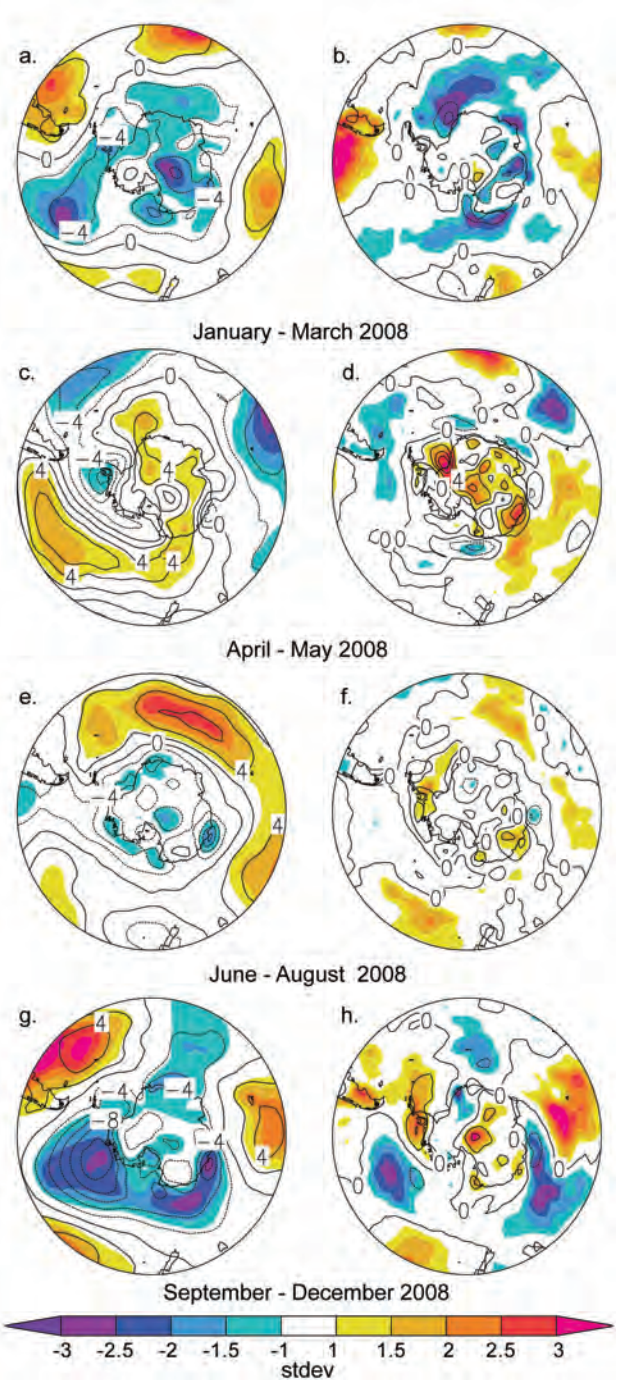


**Fig. 6.3. (left) Surface pressure anomalies and (right) surface temperature anomaly contours relative to 1979–2007 climatology for four distinct periods. The shaded regions correspond to the number of std devs the anomalies are from the 1979–2007 mean, as in Fig. 6.2. Data are from the NCEP–NCAR reanalysis.**

The Antarctic upper stratosphere (above 50 hPa) remained anomalously cold during the polar night, from March to September (Fig. 6.2), which allowed for high levels of polar stratospheric cloud formation (especially during the autumn). During the early and late portions of 2008, there is strong evidence that the stratosphere and troposphere were dynamically coupled during the positive phase of the SAM, as both low geopotential height and positive circumpolar wind anomalies extend up to 10 hPa.

*c. Surface station observations*—S. Colwell and J. Turner

Figure 6.4 highlights the temperature, MSLP, and wind speed anomalies at six representative Antarctic stations in 2008. Rothera (67.5°S, 68.1°W) and Marambio Base (64°S, 56°W) are situated along the west and east sides of the Antarctic Peninsula, respectively; Halley V Station (75°S, 26°W) lies in the Weddell Sea region of West Antarctica; Davis (68.6°S, 78.0°E) and Dumont d'Urville (66.7°S, 140.0°E) are in coastal East Antarctica; and McMurdo Station (77°S, 166°E) lies more inland near the junction of the Ross Ice Shelf/Ross Sea. All-time record anomalies are highlighted with plus signs in Fig. 6.4, while asterisks mark the second-highest anomaly. Station records extend back until at least the 1970s, although most extend to 1956–57 (see caption for details).

In January, record cold was observed at Halley, and at McMurdo the MSLP was the second lowest. At Dumont d'Urville a mean monthly minimum tem-

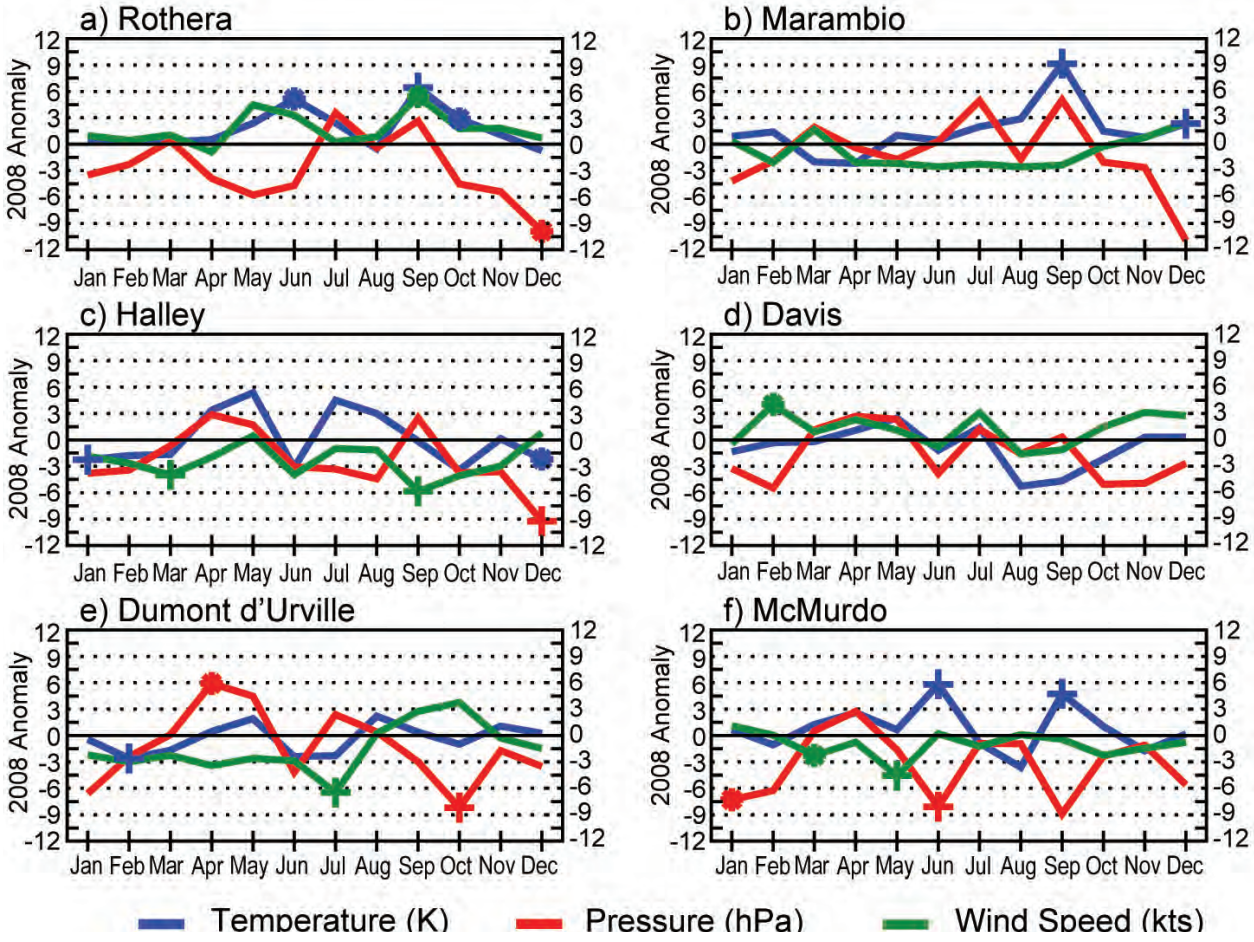


**Fig. 6.4. 2008 Antarctic station anomalies. Monthly mean anomalies for temperature (K), MSLP (hPa), and wind speed (m $s^{-1}$) are shown for six representative stations. Plus signs denote all-time record anomalies, while asterisks denote the second-highest record anomaly for each station. Climatological station data starts in 1976 for Rothera; 1970 for Marambio (1983 for Marambio wind speeds); and 1956–57 for the other stations. The base period for calculating the anomalies was 1979–2007 for all but Rothera, where the base period was 1976–2007.**

perature of −6.7°C was recorded in February, 0.8°C colder than any previous February value. Although winds were anomalously weak at Halley in March and at McMurdo from March through May, the only other notable anomaly in March–May across all stations was the second-highest pressure at Dumont d'Urville in May. During the June SAM maxima, MSLP was at a record low at McMurdo, confirmed in the more complete Scott Base record (which is within a few kilometers). At the same time, temperatures there were at a record high, opposite of the pronounced cooling expected in interior Antarctica during positive SAM phases (Marshall 2007). However, Rothera observed the second-warmest June, consistent with the impact of the positive SAM.

There were many record anomalies from August through October. In September the temperature at Rothera was 1.8°C above the previous highest September value and more than 6°C above normal (Fig. 6.4a). At Marambio the mean temperature was 2.3°C above the previous highest September mean and 9°C above normal (Fig. 6.4b); anomalously warm conditions were also observed at McMurdo in September (Fig. 6.4f). At Davis in East Antarctica the temperatures were colder than average (but not a record) in August, September, and October (Fig. 6.4d).

There is also some reflection of the positive SAM in December. Rothera observed the second-lowest pressure anomaly in December since the record began in 1976. At Marambio, the December temperature was the warmest on record, while December temperatures were the second coldest at Halley and pressures were the record lowest.

*d. Surface mass balance*—D. H. Bromwich, S.-H. Wang, and A. J. Monaghan

Precipitation-minus-evaporation (P–E) closely approximates the surface mass balance over most of Antarctica, with precipitation being the dominant term at regional and larger scales, especially near the coast (e.g., Bromwich et al. 2004; van den Broeke et al. 2006). Precipitation and evaporation fields from the JRA (Onogi et al. 2005) and NCEP–DOE Reanalysis II (NCEP2; Kanamitsu et al. 2002) were examined to assess Antarctic snow accumulation for 2008. The evaporation in JRA was calculated from the surface latent heat flux. Both JRA and NCEP2 (not shown) give similar findings. The mass balance is summarized by the annual mean and spring (SON) P–E anomalies (Fig. 6.5; anomalies are calculated from the 1980–2007 average), as the spring season dominates the annual mean, especially over the Antarctic Peninsula.

In general, the annual anomalies (Fig. 6.5a) over the high interior of the continent are small and negative. However, most coastal regions have positive anomalies, especially the Antarctic Peninsula (~400 mm) and near Casey (~700 mm) at 110° E. The annual P–E anomalies are consistent with the mean atmospheric circulation dominated by the SON MSLP anomalies (Fig. 6.3g): two strong negative pressure anomaly centers (~105° W and ~120° E) produced higher-than-normal precipitation in these regions. Negative P–E anomalies are observed over the Amundsen Sea and the Antarctic coast between 140° E and 180°. Both are linked to the secondary negative anomaly of MSLP near 180° longitude.

Over the Antarctic Peninsula the SON anomalies (~175 mm) contribute nearly 50% of annual P–E anomalies. The strong negative MSLP anomaly pattern over the Amundsen Sea (Fig. 6.3g, <2.5 std devs from the mean) indicates greater-than-normal storm activity during the 2008 SON season that results in the large P–E anomaly. As noted in section 6b, the enhanced SON storm activity is consistent with strong positive anomalies of both the SAM and La Niña during austral spring 2008.

*e. Seasonal melt extent and duration*—L. Wang and H. Liu

The extent, onset date, end date, and duration of snowmelt on the Antarctic ice sheet during 2007–08 summer was derived using a wavelet-transform-based edge detection method (Liu et al. 2005). The 19-GHz horizontal polarization channel of SSM/I data are utilized for the melt information extraction. Figure 6.6 shows the melt extent and duration during the austral

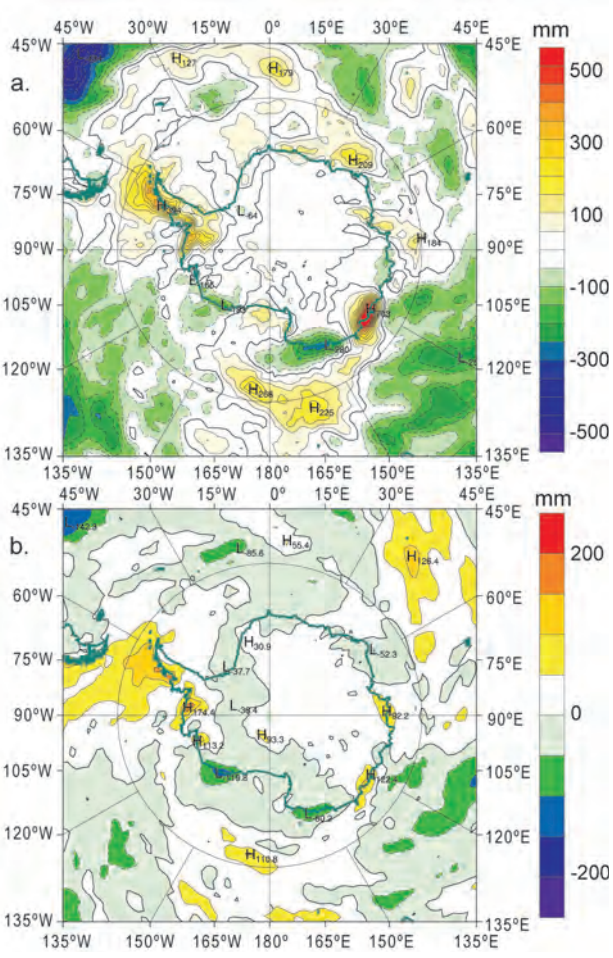


**Fig. 6.5. JRA 2008 anomalies of P−E (in mm) from the 1980–2007 average: (a) annual and (b) spring (SON).**

summer 2007–08. The total melt extent, including all areas with at least one day of surface melting, is 800,000 km$^2$, covering only 5.8% of the continent (Figs. 6.6a–c). The melt index (sum of total melt extent for each day in the melt season) during 2007–08 is 24,353,750 day km$^2$. The melt extent during 2007–08 is significantly smaller than the average melt extent (1.277 million km$^2$) of the past 25 years, or 9.34% of the continent's area (Liu et al. 2006). This places the austral summer of 2007–08 as the second lowest since 1978 in terms of both melt extent and melt index, behind only the 1999–2000 melt season. Also, it should be noted that a decreasing trend in melt extent and melt index is apparent for the past six years.

Surface melt during 2007–08 primarily occurred on the Antarctic Peninsula, Abbot Ice Shelf, West Ice Shelf, and Shackleton Ice Shelf (see Fig. 6.6 for locations). Surface melt events primarily took place in December and January (Figs. 6.6a,b,d), and the maximum one-day melt extent occurred on 21 December. All the regions in Antarctica have a considerably

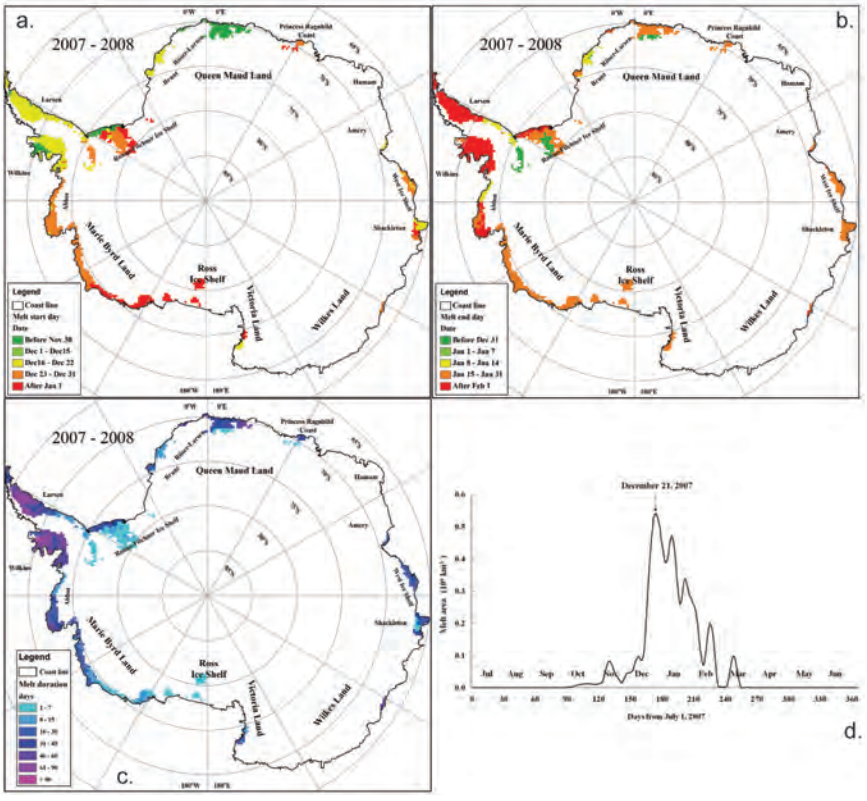


**Fig. 6.6. Surface snow (a) onset date, (b) end date, (c) duration in days, and (d) melt area, for the austral 2007–08 melt season.**

lower melt extent than the average of the past 25 years, which is consistent with weak surface cold temperature anomalies in December 2007 (Fig. 6.2) and January 2008 (Fig. 6.4). The Amery Ice Shelf, Queen Maud Land, Wilkes Land, and Ross Ice Shelf have an extremely low melt extent and melt intensity, which is likely associated with the strong positive sea-ice extent anomalies in these regions and the influence of the strong positive SAM and 2007–08 La Niña event.

*f. Sea-ice extent and concentration*—R. A. Massom, P. Reid, S. Stammerjohn, and S. Barreira

2008 was a year of exceptional seasonal variability in Antarctic sea-ice coverage, characterized by three distinct phases of overall sea-ice extent anomalies: i) well above average (January–April inclusive and December), ii) moderately above average (May–June), and iii) average to slightly below average (July–November), but with substantial regional variability that reflects patterns of atmospheric circulation.

The analysis is based on monthly mean Nimbus-7 SMMR (1979–87) and DMSP SSM/I (1987–present) sea-ice concentration data from the NSIDC Sea Ice Index project (Fetterer et al. 2008). Note that 2008 data are processed from a combination of NSIDC's preliminary (Meier et al. 2006) and NRTSI data that have lower quality control, but they must be used because the quality-controlled data are unavailable at the time of writing. According to Fetterer et al. (2008), however, this effect is likely to be of the order of less than 10,000 km$^2$.

Monthly ice extent and concentration anomalies for 2008 display a distinct zonal asymmetry (Figs. 6.7a–d), largely in response to the location and intensity of climatological low and high pressure centers described in the atmospheric circulation section. The January–April period was characterized by the persistence of anomalously high sea-ice concentrations in the Weddell Sea and almost the entire zone from the Indian Ocean through the western Pacific Ocean and western Ross Sea sectors (from ~40°E eastward to ~160°W; Figs. 6.7a,b), resulting in record and near-record zonally averaged monthly ice extents during January–April. With an ice extent anomaly of 3.4 std devs (+33% or $1.7 \times 10^6$ km$^2$) above the long-term (1979–2000) mean of $5.1 \times 10^6$ km$^2$, January 2008 continued from December 2007 as being a record high for that month (Fig. 6.7e), that is, ~11% greater than the previous record high for January (in 1996). Major positive anomalies of +28% occurred in both February and March (3.31 and 3.16 std devs above the mean, respectively) and +18% in April (2.27 std devs above the mean). Record monthly high values were also recorded in March and April: the March 2008 anomaly exceeded the previous record (in 2001) by about 10%, and April was about 5% greater than the previous highs in 1979 and 1982 (Fig. 6.7f). February 2008 saw the second-highest monthly sea-ice extent on record. The persistence of unusually compact sea ice in many regions into the summer melt period led to difficulties in ship navigation during the critical shipping (base resupply) and tourist season of early 2008 (especially in accessing the Ross Sea). More

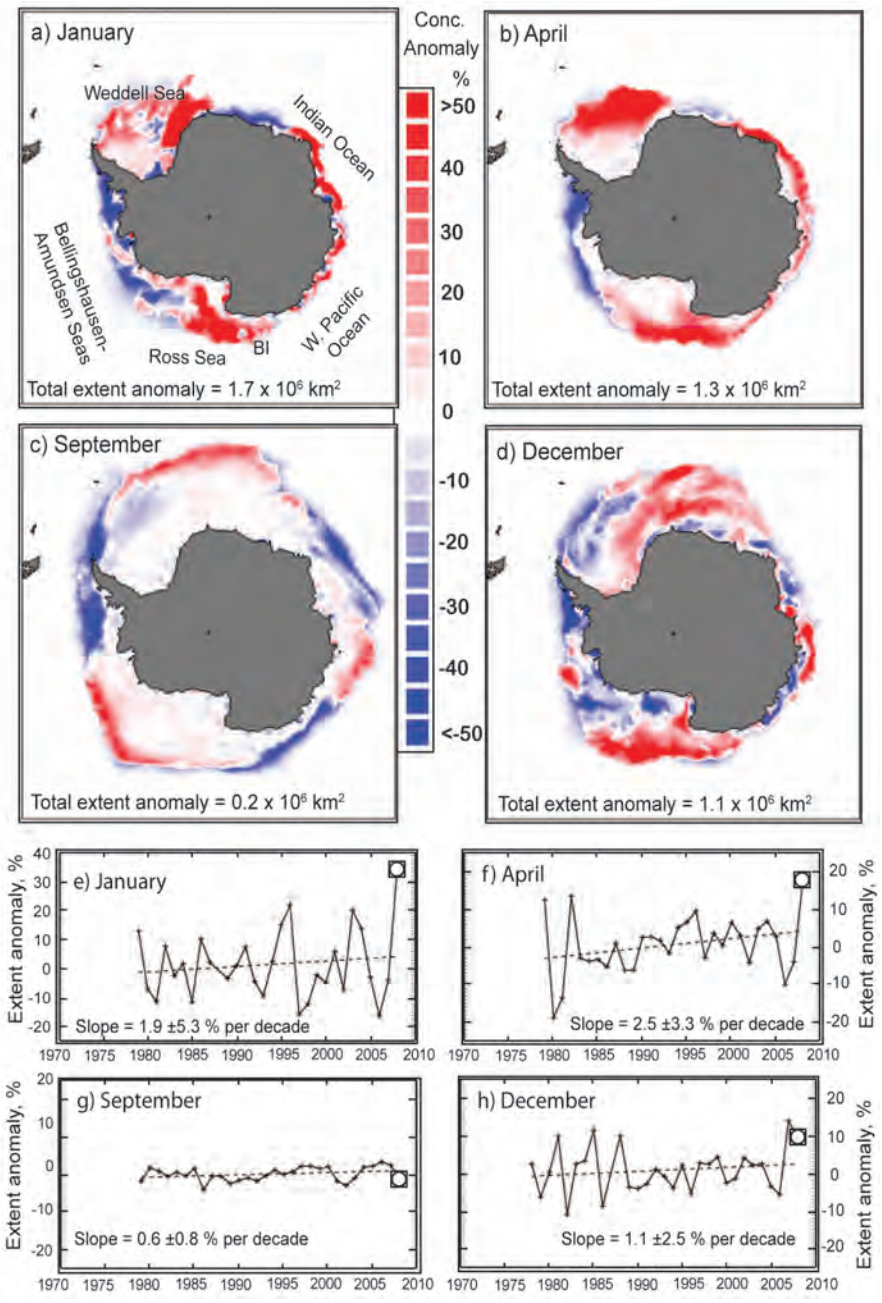


**Fig. 6.7. Antarctic sea-ice extent and concentration anomalies for (a) Jan, (b) Apr, (c) Sep, and (d) Dec, and coincident trends in (e–h) sea-ice extent, all for 2008. The bold black line represents the long-term monthly mean sea ice extent (1979–2000) for that particular month, while the dashed black line is the monthly mean for the month in 2008 (both equivalent to the 15% ice concentration isoline). The ice concentration anomaly is computed from the monthly mean ice concentration relative to the long-term mean (1979–2000) for that particular month. The ice concentration anomaly is only calculated for the area covered by sea ice for the month (in 2008) in question. BI is Balleny Islands.**

extensive sea ice also occurred in the May–June period (late autumn to early winter), but at lower levels compared to the previous four months.

In contrast, sea-ice extent was generally close to (i.e., within ±2%) the long-term mean for July through November, although it was again characterized by marked regional variability. Negative anomalies in the Amundsen/Bellingshausen and northwest Weddell Seas, the Indian, and west Pacific Ocean sectors were compensated for by positive anomalies in the northeast Weddell and Ross Sea sectors. The sea-ice extent during December, $12.2 \times 10^6$ km$^2$, was well above the long-term average of $11.1 \times 10^6$ km$^2$.

A major feature throughout the year is anomalously low sea-ice extent for every month in the Bellingshausen/Amundsen Seas (west Antarctic Peninsula) sector. This represents a continuation in the long-term trend in this region (Stammerjohn et al. 2008). The juxtaposition of this major sea-ice "indentation" to strong positive (ice growth) anomalies in the adjacent Ross Sea sector is largely due to the dominant impact of surface winds associated with a persistent deep low pressure system centered on approximately 240°E, 68°S (the "Amundsen Sea Low"; Fig. 6.3g). This leads to sustained west-northwesterly airflow across the west Antarctic Peninsula sector to hold back autumnal ice-edge advance and accelerate the spring retreat, causing dynamic sea-ice compaction against the coast and islands (Massom et al. 2008). It is most strongly seen in 2008 during October and November. By the same token, the more southerly outflow of cold air from continental Antarctica along the western flank of this system

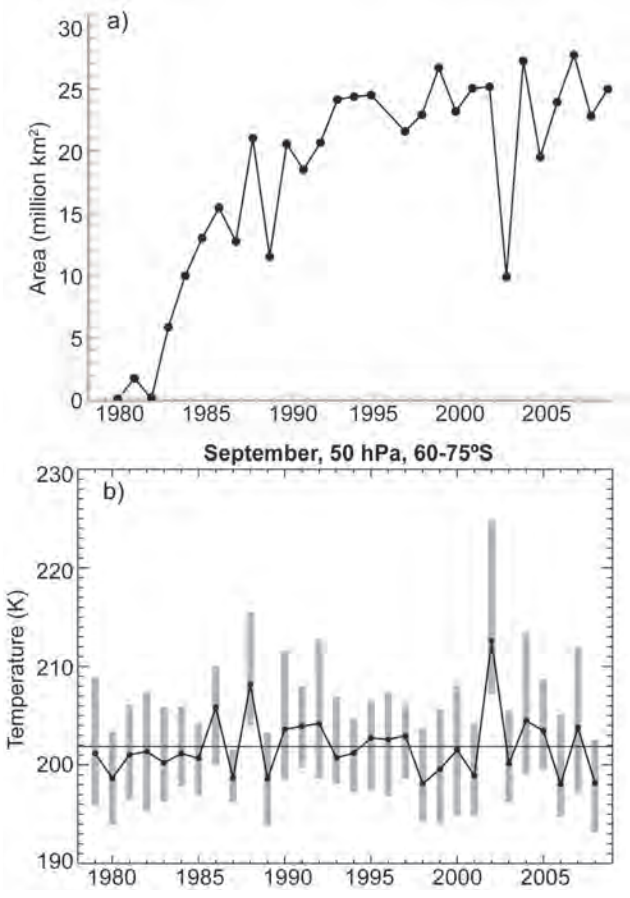


**Fig. 6.8. (a) Ozone hole area, 1979–2008. The area is calculated by first calculating the area enclosed by the 220 DU value over the Southern Hemisphere for each day from 21 to 30 Sep, and then averaging these 10 days. The area of the North American continent is indicated by the horizontal bar (24.71 million km$^2$). (b) Temperature at 50 hPa from 60° to 75°S during Sep 1979–2008. The vertical bars represent the range of values from the individual days of Sep. The Sep average over the 1979–2008 period is indicated by the horizontal line.**

creates a strong ice-edge advance, and in 2008 led to a positive ice concentration and extent anomaly across the Ross Sea sector from April through December. The increased occurrence of an intensified Amundsen Sea Low is contemporaneous with an increase and poleward shift of the westerly circulation in the high-latitude South Pacific, which happened in 2008 in response to La Niña and/or positive SAM conditions, as well as a wave-3 atmospheric circulation pattern. Finally, the 2008 continuation of decreased sea ice in the Amundsen/Bellingshausen Seas is particularly noteworthy given the recent association of the decreasing regional trend with amplified surface warming of the West Antarctic ice sheet during the last 30 years (Steig et al. 2009).

*g. Ozone depletion*—P. A. Newman

Analysis of the 2008 ozone concentrations is based on data from the NASA Aura satellites, in particular, the KNMI OMI and the JPL MLS. PSC information was obtained from the NASA LaRC CALIPSO instrument. NOAA/NCEP provided analyses of satellite and balloon stratospheric temperature observations. NOAA/ESRL regularly launches ozone- and temperature-measuring balloon instruments from the South Pole. Figure 6.8a displays the average area of the Antarctic ozone hole from 1979 to 2008, estimated by first summing the area of the daily total column ozone values less than 220 DU from the Aura OMI observations, and then averaging these estimates from 21–30 September. Based on these measurements, the Antarctic ozone hole was the sixth worst on record for 2008, fifth worst when using SBUV total ozone from the NOAA polar orbiter satellites. The area of the hole was approximately 25 million km$^2$ (9.65 million mi$^2$), somewhat smaller than the 2006 record of 27.7 million km$^2$ (10.7 million mi$^2$). The very large ozone hole area is consistent with severe depletion caused by the high levels of chlorine and bromine in the Antarctic stratosphere. At present, ODSs are estimated to have only decreased by about 4% from the peak levels in the 2000–02 period.

The total ozone values over Antarctica steadily decreased from July to early October 2008. Aura OMI observations showed ozone values of about 230 DU near the edge of Antarctica (inside the stratospheric polar vortex in early July) and a low value of 100 DU on 4 October 2008. Balloon-borne ozonesonde observations from NOAA/ESRL at the South Pole also showed similar behavior. On 22 August total ozone estimated from these sondes was 260 DU, with a decrease to 107 DU on 28 September. The ozonesonde profile information showed that the large losses occurred in the lower stratosphere by late September, with a near complete loss of ozone in the 14–20-km layer on 8 October.

Figure 6.8b shows the temperature average (based on the NCEP–NCAR reanalysis) for September at 50 hPa averaged from 60°–75°S (edge of the polar vortex). The September 2008 period was nearly the coldest on record, but comparable to 1980, 1987, 1989, 1998, and 2006. The cold temperatures result in an increased frequency of PSCs, where chlorine molecules are converted from their nonreactive forms into their reactive forms; the latter leads to rapid ozone destruction. In terms of season-integrated totals, CALIPSOs indicate that the 2008 season PSC volume started on par with the record 2006 season but dropped off significantly in August. The overall PSC volume in

2008 ended about 16% lower than in 2006 (Pitts et al. 2009). The cold stratospheric temperatures in winter and spring (Fig. 6.2b), particularly in September 2008 (Fig. 6.8b), were due to weaker-than-normal (5% below the average for the August–September period) wave activity.

The 2008 ozone hole was unusually persistent, with low ozone values extending into the late-December period. The Antarctic ozone hole causes the spring-like conditions to persist because the ozone-depleted air cannot absorb shortwave radiation. Hence, temperatures in the Antarctic spring and early summer are colder, and the vortex transitions to summer conditions at a later date. In addition, lack of wave forcing to dynamically warm the stratosphere can lead to colder spring conditions. In November 2008, ozone depletion combined with a lack of wave driving to produce a cold and stable vortex that persisted well into the December period (Fig. 6.2b). In fact, the polar vortex in 2008 persisted beyond any previous year dating to 1979. Consequently, the area of depleted ozone below 220 DU also persisted to the latest date.